# Observed and Simulated Summer Rainfall Variability in Southeastern South America

**Leandro B. Díaz, Carolina S. Vera, Ramiro I. Saurral**

Centro de Investigaciones del Mar y la Atmósfera/CONICET-UBA DCAO/FCEN, UMI-IFAECI/CNRS, Buenos Aires, Argentina

***Contact e-mail:*** *ldiaz@cima.fcen.uba.ar*

## Introduction

The climate changes observed in the last decades have raised concern among policy and decision makers about the importance of improving the knowledge and prediction of climate. In particular, the Southeastern South America (SESA) is one of the few regions in the world which have experimented both large positive summer precipitation trends in mean and extremes during the 20th century (e.g. Liebmann et al., 2004; Re and Barros, 2009; Penalba and Robledo, 2010; Saurral et al., 2016). Furthermore, a precipitation increase is projected over the region for the current century (Hartmann et al., 2013). These changes pose a significant threat for many socio-economic sectors within this region.

Recently, Vera and Díaz (2015) have shown that the fifth phase of the Coupled Model Intercomparison Project of the World Climate Research Program (CMIP5, Taylor et al., 2012) multi-model historical simulation dataset (i.e. including all observed forcings) is able to represent the sign of the trends of the last century over SESA, although with a weaker magnitude. When comparing results from the historical simulation including all forcings against those only including natural forcings and only considering greenhouse gases forcing, they concluded that anthropogenic forcing in CMIP5 models has a detectable influence in explaining the observed positive precipitation trends.

Through teleconnection patterns, tropical ocean variability is one of the main precipitation forcings in SESA. The El Niño Southern Oscillation (ENSO) has been shown to be the main influence for SESA rainfall variability on interannual scales (e.g. Ropelewski and Halpert, 1987; Kiladis and Diaz, 1989). However, the way in which ENSO affects SESA rainfall seems to be modulated by ocean lower-frequency patterns as the Pacific Decadal Oscillation (PDO) (Kayano and Andreoli, 2007) and the Atlantic Multidecadal Oscillation (AMO) (Kayano and Capistrano, 2014). Furthermore, Barreiro et al. (2014) found that both, PDO and AMO, have also an influence on summer SESA rainfall independently from ENSO.

How anthropogenic forcings are combined with low frequency natural climate variability to modulate the regional rainfall variability and trends in SESA has not been explored in detail yet. Therefore, a deeper knowledge of decadal climate variability in the region is needed in order to project near term future changes with a larger degree of confidence. According to this, our goal is to understand the influence of the large-scale interannual variability of sea surface temperatures (SST) on austral summer rainfall in SESA in a global warming context and to evaluate if CMIP5 models are able to represent that influence properly.

## Leading observed co-variability pattern of SST and SESA rainfall

Rainfall data from the Global Precipitation Climatology Centre (GPCC) dataset (Schneider et al., 2011) were used in this study, with a spatial resolution of 2.5°. This product considers station-based records, and thus it only has continental coverage. SST monthly values were derived from the NOAA Extended Reconstructed Sea Surface Temperature Version 3b (ERSSTv3b, Smith et al., 2008) with a spatial resolution of 2°. Summer was defined as the December–January–February (DJF) trimester. Anomalies were computed from the corresponding long-term means considering the period 1902–2010. Both undetrended and detrended anomalies were defined for both variables. Non-linear trends were removed through a linear regression between global mean SST time series and those for SST or precipitation anomalies at each grid point. Removing linear trends instead of non-linear produce slightly different results in variability patterns obtained, especially for higher order modes. As global warming trend is non-linear, the removal of non-linear trends allows to better identified variability beyond the global warming signal.

The influence of the observed large-scale interannual variability of the SST anomalies on austral summer rainfall in SESA is described through a singular value decomposition analysis (SVD) performed jointly on the summer seasonal rainfall anomalies over SESA

(39°S-16°S;64°W-31°W) and SST anomalies from 45°N to 45°S. The temporal variability of each mode is described by the time series of the expansion coefficients (hereinafter SVD time series) resulted for each variable from the SVD analysis. Correlation maps between the SVD time series of SST and SST anomalies at each grid point (i.e. homogeneous correlation map) were computed to describe the SST patterns associated with the modes. On the other hand, the correlation maps between the SVD time series of SST and precipitation anomalies at each grid point (i.e. heterogeneous correlation map) were used to describe the mode influence on precipitation in southern South America.

The temporal series of the first mode (SVD1), which accounts for 71% of the total squared covariance, exhibits significant variability on interannual timescales, modulated by long-term trends (Fig 1a). The mode is positively correlated with SST anomalies almost everywhere with maximum values in the tropical portions of the Pacific and Indian Oceans (Fig 1b). It also exhibits positive correlations with rainfall anomalies in northern Argentina, Uruguay and Southern Brazil (Fig 1c).

The SVD analysis was also performed considering the detrended anomalies of both variables. The corresponding SVD1 accounts for 51% of the total squared covariance and it presents a strong decadal modulation of its year-to-year activity with phase shifts at around the 1930s, 1970s and 1990s (Fig 1d). This mode shows positive correlations with rainfall anomalies in SESA (Fig 1f) and SST anomalies in equatorial Pacific and Indian Oceans (Fig 1e). Moreover, the mode presents negative correlations with SST anomalies in the North and South Pacific distributed in a 'horseshoe-like' spatial pattern resembling that associated with ENSO or the PDO. A similar SST and precipitation correlation pattern was identified by Grimm (2011) for the second variability mode of summer precipitation for the period 1961-2000, considering almost all South America. Furthermore, the characteristics of the SVD1 obtained here are also similar to the ones obtained by Robledo et al. (2013), computing a SVD analysis between global SST anomalies and daily precipitation extreme index in SESA.

The SVD time series resulting from the analysis of both undetrended and detrended anomalies (Fig 1a and Fig 1d, respectively) shows periods in which the expansion coefficients of the two variables are in phase, while in others they are not. The correlation between those two series can be considered a measure of the strength of the coupling between SST and precipitation patterns obtained from SVD1 (e.g. Venegas et al., 1997). Then, in order to explore changes in the coupling between global SST and SESA rainfall, a 19-year sliding correlation analysis was performed to the SVD time series resulting from the undetrended and detrended anomalies of both variables. Fig 2 shows that sliding correlations are positive for all the period considered, although decadal variations are noticeable. Periods of high coupling (1930s-1940s, 1990s) and low coupling (1980s) can be identified. The results agree with those obtained by Martín-Gómez et al. (2016) using a complex network methodology to detect synchronization periods among the tropical oceans and the precipitation over SESA. In general, sliding correlations are higher for the detrended case (Fig 2), indicating that trends for both variables show different behaviour in some periods, which reduce the corresponding correlation. Preliminary exploratory analysis (not shown) for the detrended case suggest that during positive (negative) events of SDV1, defined as those years in which the SVD1 time series for SST is above 1 (below -1), negative (positive) Southern Annular Mode (SAM) phases seem to reinforce the teleconnections, induced by the tropical Pacific-Indian ocean conditions, in the vicinity of South America. The SAM influence on the Pacific teleconnection has been proposed earlier by Vera et al. (2004) and Fogt and Bromwich (2006).

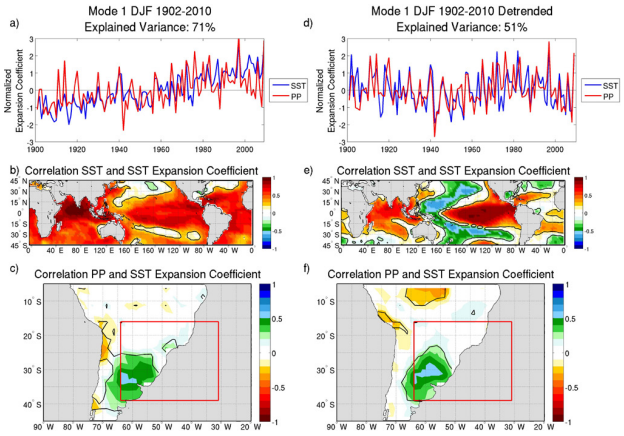


**Figure 1: (a)** SVD time series of SST (blue) and rainfall anomalies (red) over SESA (region indicated by the red rectangle in c). **(b)** Homogeneous correlation map between the SVD time series of SST and SST grid point anomalies. **(c)** Heterogeneous correlation map between the SVD time series of SST and rainfall grid point anomalies. **(d)**, **(e)** and **(f)** same as (a), (b) and (c), but for the detrended anomalies. Contours indicate 95% significance level.

## Leading simulated co-variability pattern of SST and SESA rainfall

A preliminary evaluation of coupled general circulation models' ability in representing the main SVD1 features was made. Historical simulations from 39 models included in CMIP5 were considered. The simulated spatial SVD1 patterns obtained from detrended anomalies were computed over the period 1902-2005 (available period for both observations and models), and compared with those resulted from the observed datasets. An index (M) was defined as the spatial correlation between the simulated and observed patterns for SST, times the spatial correlation between the simulated and observed patterns

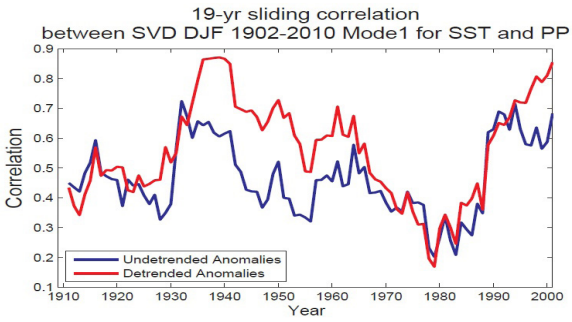


**Figure 2:** 19-year sliding correlation between SVD time series for SST and rainfall anomalies over SESA for the undetrended (blue) and detrended (red) anomalies.

for rainfall. If M is close to 1, both SST and precipitation patterns are represented properly by the models, while values close to 0 or negatives indicate that models fail in representing properly the observed patterns. To obtain the model ensemble mean, mean of M for each model is computed over all of their members. Inter model dispersion are described by the corresponding standard deviation.

Some CMIP5 models are able to reproduce the spatial patterns corresponding to the leading mode of co-variability, although other are not skillful (Fig 3). The M index value averaged over all models is 0.35, with 25 models from a total of 39, with M values above it. Inter member dispersion is highly variable between models. For some models, like GISS-E2_H, IPSL-CM5A-LR or NorESM1-M, M value could be positive, negative or close to zero depending on the realization selected. In other models, like CCSM4 or HadGEM2-ES, an outlier member mostly affects model performance. On the other hand, there are models that have high M values and low inter member dispersion, as CanESM2, CNRM-CM5, GFDL-CM3 or GISS-E2-R. On average, most models tend to represent properly the SST pattern corresponding to SVD1, with a mean correlation value of 0.69 ranging between 0.32 and 0.9. However, the representation of the rainfall pattern in SESA region is less satisfactory, associated with mean correlation values of 0.45, but extended between -0.75 and 0.82. Several models tend to reproduce a dipole rainfall correlation pattern in southern South America, instead of the observed monopole. These results allows us to conclude that most models in CMIP5 historical simulations are able to reproduce reasonably well the spatial leading pattern of co-variability between SST and SESA rainfall.

## Concluding remarks

The co-variability between global SST anomalies and precipitation anomalies in SESA during summer was assessed through a SVD analysis over the period 1902-2010. The temporal series of the SVD1 exhibits significant variability on interannual timescales, modulated by long-term trends. The mode is positively correlated with SST anomalies almost everywhere with maximum values in

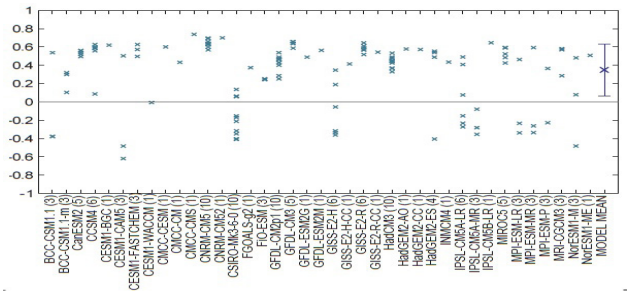


**Figure 3:** M index (see text for details) for WCRP/CMIP5 models members and model mean. Brackets indicate number of members for each model. Blue bar indicate inter model dispersion for model ensemble mean.

the tropical portions of the Pacific and Indian Oceans, and also exhibits positive correlations with rainfall anomalies in SESA. When detrended anomalies of both variables were considered, the corresponding SVD1 temporal series presents a strong decadal modulation of its year-to-year activity. The corresponding mode shows positive correlations with rainfall anomalies in SESA and SST anomalies in equatorial Pacific and Indian Oceans, and negative correlations with SST anomalies in the North and South Pacific distributed in a 'horseshoe-like' spatial pattern resembling that associated with ENSO or the PDO. Periods of high coupling (1930s-1940s, 1990s) and low coupling (1980s) between undetrended and detrended anomalies of both variables could be identified.

A preliminary analysis of CMIP5 models representation of SVD1 was also performed. Most models in CMIP5 historical simulations are able to reproduce reasonably well the spatial leading pattern of co-variability between SST and SESA rainfall. The reasonable ability that many CMIP5 models exhibits in representing the global SST influence on summer precipitation in SESA, suggests that some model prediction skill might be obtained by simulations that account for a proper initialization of the ocean. Recently, it has been shown that the CMIP5 decadal predictions have some predictive skill in different ocean basins for a few years (e.g. Meehl et al., 2014). As a consequence, future research will be advocated to the evaluation of the decadal predictability of the SST anomalies in those regions influencing SESA rainfall.

## Acknowledgments

Leandro Diaz acknowledges the World Climate Research Programme (WCRP) for funding his assistance to the CLIVAR Open Science Conference (Qingdao, 2016), where this work has been awarded. The research was supported by Consejo Nacional de Investigaciones Científicas y Técnicas (CONICET) PIP 112-20120100626CO, UBACyT 20020130100489BA, PIDDEF 2014/2017 Nro 15, andthe CLIMAX Project funded by Belmont Forum. Leandro Díazwas supported by a PhD grant from CONICET, Argentina.

## References


Barreiro, M., N. Díaz, and M. Renom, 2014: Role of the global oceans and land-atmosphere interaction on summertime interdecadal variability over northern Argentina. Clim. Dyn., 42, 1733–1753, doi:10.1007/s00382-014-2088-6.

Fogt, R. L., and D. H. Bromwich, 2006: Decadal variability of the ENSO teleconnection to the high-latitude south pacific governed by coupling with the Southern Annular mode. J. Clim., 19, 979–997, doi:10.1175/JCLI3671.1.

Grimm, A. M., 2011: Interannual climate variability in South America: Impacts on seasonal precipitation, extreme events, and possible effects of climate change. Stoch. Environ. Res. Risk Assess., 25, 537–554, doi:10.1007/s00477-010-0420-1.

Hartmann, D. L., and Coauthors, 2013: Observations: Atmosphere and surface. Climate Change 2013: The Physical Science Basis, T. F. Stocker et al., Eds., Cambridge University Press, 159–254.

Kayano, M. T., and R. V. Andreoli, 2007: Relations of South American summer rainfall interannual variations with the Pacific Decadal Oscillation. Int. J. Climatol., 27, 531–540, doi:10.1002/joc.1417.

Kayano, M. T., and V. B. Capistrano, 2014: How the Atlantic multidecadal oscillation (AMO) modifies the ENSO influence on the South American rainfall. Int. J. Climatol., 34, 162–178, doi:10.1002/joc.3674.

Kiladis, G. N., and H. F. Diaz, 1989: Global Climatic Anomalies Associated with Extremes in the Southern Oscillation. J. Clim., 2, 1069–1090, doi:10.1175/1520-0442(1989)002<1069:GCAAWE>2.0.CO;2.

Liebmann, B., C. Vera, L. Carvalho, I. Camilloni, M. Hoerling, D. Allured, V. Barros, J. Báez, and M. Bidegain, 2004: An Observed Trend in Central South American Precipitation. J. Climate, 17, 4357–4367, doi: 10.1175/3205.1.

Martín-Gómez, V., E. Hernández-Garcia, M. Barreiro, and C. López, 2016: Interdecadal Variability of Southeastern South America Rainfall and Moisture Sources during the Austral Summertime. J. Climate, 29, 6751–6763, doi: 10.1175/JCLI-D-15-0803.1.

Meehl, G., L. Goddard, G. Boer, R. Burgman, G. Branstator, C. Cassou, S. Corti, G. Danabasoglu, F. Doblas-Reyes, E. Hawkins, A. Karspeck, M. Kimoto, A. Kumar, D. Matei, J. Mignot, R. Msadek, A. Navarra, H. Pohlmann, M. Rienecker, T. Rosati, E. Schneider, D. Smith, R. Sutton, H. Teng, G. van Oldenborgh, G. Vecchi, and S. Yeager, 2014: Decadal Climate Prediction: An Update from the Trenches Bull. Amer. Meteor. Soc., 95, 243–267, doi: 10.1175/BAMS-D-12-00241.1.

Penalba, O. C., and F. A. Robledo, 2010: Spatial and temporal variability of the frequency of extreme daily rainfall regime in the La Plata Basin during the 20th century. Clim. Change, 98, 531–550, doi:10.1007/s10584-009-9744-6.

Re, M., and V. R. Barros, 2009: Extreme rainfalls in SE South America. Clim. Change, 96, 119–136,doi:10.1007/s10584-009-9619-x.

Robledo, F. A., O. C. Penalba, and M. L. Bettolli, 2013: Teleconnections between tropical-extratropical oceans and the daily intensity of extreme rainfall over Argentina. Int. J. Climatol., 33, 735–745, doi:10.1002/joc.3467.

Ropelewski, C. F., and M. S. Halpert, 1987: Global and Regional Scale Precipitation Patterns Associated with the El Niño/Southern Oscillation. Mon. Weather Rev., 115, 1606–1626, doi:10.1175/1520-0493(1987)115<1606:GARSPP>2.0.CO;2.

Saurral, R. I., I. A. Camilloni, and V. R. Barros, 2016: Low-frequency variability and trends in centennial precipitation stations in southern South America. Int. J. Climatol., doi:10.1002/joc.4810.

Schneider, U., A. Becker, P. Finger, A. Meyer-Christoffer, B. Rudolf, and M. Ziese, 2011: GPCC Full Data Reanalysis Version 6.0 at 2.5°: Monthly Land-Surface Precipitation from Rain-Gauges built on GTS-based and Historic Data, doi: 10.5676/DWD_GPCC/FD_M_V7_250

Smith, T. M., R. W. Reynolds, T. C. Peterson, and J. Lawrimore, 2008: Improvements to NOAA's historical merged land-ocean surface temperature analysis (1880-2006). J. Clim., 21, 2283–2296, doi:10.1175/2007JCLI2100.1.

Taylor, K. E., R. J. Stouffer, and G. A. Meehl, 2012: An overview of CMIP5 and the experiment design. Bull. Am. Meteorol. Soc., 93, 485–498, doi:10.1175/BAMS-D-11-00094.1.

Venegas, S. A., L. A. Mysak, and D. N. Straub, 1997: Atmosphere-ocean coupled variability in the South Atlantic. J. Clim., 10, 2904–2920, doi:10.1175/1520-0442(1997)010<2904:AOCVIT>2.0.CO;2.

Vera, C., G. Silvestri, V. Barros, and A. Carril, 2004: Differences in El-Niño response over the southern hemisphere. J. Clim., 1741–1753, doi:10.1175/1520-0442(2004)017<1741:DIENRO>2.0.CO;2.

Vera, C. S., and L. Díaz, 2015: Anthropogenic influence on summer precipitation trends over South America in CMIP5 models. Int. J. Climatol., 35, 3172–3177, doi:10.1002/joc.4153.